Research Paper

Disease-specific primed human adult stem cells effectively ameliorate experimental atopic dermatitis in mice

Byung-Chul Lee[1], Jae-Jun Kim[1], Jin Young Lee[1], Insung Kang[1,§], Nari Shin[1], Seung-Eun Lee[1], Soon Won Choi[1], Je-Yoel Cho[2], Hyung-Sik Kim[3,4✉*], Kyung-Sun Kang[1✉*]

1. Adult Stem Cell Research Center and Research Institute for Veterinary Science, College of Veterinary Medicine, Seoul National University, Seoul 08826, Republic of Korea
2. Department of Biochemistry, BK21 PLUS Program for Creative Veterinary Science Research and Research Institute for Veterinary Science, College of Veterinary Medicine, Seoul National University, Seoul 08826, Republic of Korea
3. Department of Life Science in Dentistry, School of Dentistry, Pusan National University, Yangsan 50612, Republic of Korea
4. Institute for Translational Dental Sciences, Pusan National University, Yangsan 50612, Republic of Korea

*Authors share co-corresponding authorship

§Current address: Program in Developmental Endocrinology and Genetics, Eunice Kennedy Shriver National Institute of Child Health and Human Development, NIH, Bethesda, MD 20892, USA

✉ Corresponding author: Kyung-Sun Kang, D.V.M., Ph.D. Adult Stem Cell Research Center, College of Veterinary Medicine, Seoul National University, 1 Gwanak-ro, Gwanak-gu, Seoul 08826, South Korea. Tel. +82-2-880-1246 E-mail: kangpub@snu.ac.kr Hyung-Sik Kim, D.V.M., Ph.D. Department of Life Science in Dentistry, School of Dentistry, Pusan National University, Yangsan 50612, Republic of Korea. Tel: +82-51-510-8231 E-mail: hskimcell@pusan.ac.kr

Abstract

Although human mesenchymal stem cells (hMSCs) hold considerable promise as an alternative therapeutic reagent for allergic disorders including atopic dermatitis (AD), the strategy for enhancing hMSC-based therapy remains challenging. We sought to investigate whether preconditioning with mast cell (MC) granules could enhance the therapeutic efficiency of human umbilical cord blood-derived MSCs (hUCB-MSCs) against AD.

Methods: AD was experimentally induced in NC/Nga mice by repeated applications of 4% sodium dodecyl sulfate (SDS) and *dermatophagoides farinae* (Df) extract, and preconditioned hUCB-MSCs were subcutaneously injected. The therapeutic effect was determined by gross examination and additional *ex vivo* experiments performed using blood and skin samples to determine the resolution of allergic inflammation. To explore the underlying mechanisms, several co-culture assays with primary isolated immune cells and wound closure assays were conducted.

Results: Pretreatment of MC granules enhanced the therapeutic effects of hUCB-MSCs by attenuating the symptoms of AD in an experimental animal model. MC granule-primed cells suppressed the activation of major disease-inducing cells, MCs and B lymphocytes more efficiently than naïve cells both *in vitro* and *in vivo*. Histamine-mediated upregulation of the COX-2 signaling pathway was shown to play a crucial role in suppression of the allergic immune response by MC-pretreated hUCB-MSCs. Moreover, MC pretreatment improved the wound healing ability of hUCB-MSCs.

Conclusions: Our findings indicate that pre-exposure to MC granules improved the therapeutic effect of hUCB-MSCs on experimental AD by resolving the allergic immune reaction and accelerating the tissue regeneration process more efficiently than naïve cells, suggesting a potential enhancement strategy for stem cell-based therapy.

Key words: Atopic dermatitis, Mesenchymal stem cells, Immunomodulation, Wound healing, Stem cell-based therapy

Introduction

Human mesenchymal stem cells (MSCs) have been spotlighted as a therapeutic reagent for atopic dermatitis (AD, or atopic eczema), because of their unique properties, immunomodulatory ability and

tissue regenerative capacity. In our previous studies, we demonstrated that hMSCs augmented therapeutic functions in response to Th2 cytokines and consequently mitigated AD by suppressing excessive allergic inflammation [1, 2]. Given their experimentally verified therapeutic effects, human umbilical cord blood-derived MSCs (hUCB-MSCs) are currently in clinical trials for the treatment of AD [3]. Although hUCB-MSCs could alleviate the symptoms of AD in phase I/IIa studies, we realized the necessity of a more efficient way to decrease the cost, treatment period and individual variation in subsequent clinical trials, suggesting that an enhancement strategy is needed for actual application.

Notably, various approaches for enhancing the therapeutic potential of MSCs have recently been proposed. For example, co-administration with advanced materials, including graphene oxide flakes and the immunomodulatory microparticle MIS416, could reportedly enhance the implantation of MSCs into the lesion [4, 5]. In addition, genetically engineered MSCs exhibited enhanced therapeutic effects in an AD animal model [6]. Priming with growth factors or cytokines released under an inflammatory state has also reportedly improved the therapeutic efficacy of these cells [7, 8]. However, whether pre-exposure to disease-related or disease-specific factors can enhance the therapeutic potential of hMSCs for the treatment of AD has not been reported.

Mast cells (MCs) play an important role in the pathogenesis of AD, functioning as key effectors during immediate hypersensitivity and allergic reactions. MCs can be sensitized by secreted immunoglobulin E (IgE) due to the expression of high-affinity receptors for IgE (FcεRI) on the cell surface, and IgE-bound FcεRI leads to the activation of cells following crosslinking with allergens [9]. Activated MCs subsequently secrete numerous molecules, including protein mediators, lipid mediators and cytokines, which elicit hypersensitive reactions, such as pruritus, Th2 skewing and skin inflammation [10]. MSCs infused *in vivo* exhibit their unique therapeutic function by sensing the disease-specific microenvironment. Therefore, disease-related factors, such as interleukin (IL)-1β, IL-6, IL-8 and tumor necrosis factor (TNF)-α, were employed to augment the therapeutic potential of MSCs against inflammatory diseases [11-14]. Because MC granules contain numerous disease-triggering molecules as well as the proinflammatory cytokines mentioned above, preconditioning with MC granules could be a novel method for improving stem-cell-based therapies against AD.

In the present study, we sought to investigate whether pretreatment with isolated MC contents could enhance the therapeutic potential of hUCB-MSCs in a *dermatophagoides farinae* (Df) extract-induced AD model. NC/Nga mice have frequently been employed as an experimental AD model, as they spontaneously develop severe dermatitis upon repetitive exposure to nonspecific allergens and exhibit clinical symptoms, such as erythema, edema, itching, dryness, excoriation and infiltration of allergic inflammatory cells, similar to human AD [15]. Therefore, this mouse model is vastly used to validate the therapeutic feasibility of alternative drugs [1, 16, 17]. Furthermore, we elucidated the mechanisms by which MC granules efficiently improve the suppressive effects of hUCB-MSCs on activated immune cells and tissue regeneration.

Methods

Isolation and culture of hUCB-MSCs

All experimental procedures using human cord blood derivatives, including hUCB-MSCs, were conducted under guidelines approved by the Boramae Hospital Institutional Review Board (IRB) and the Seoul National University IRB (IRB no. 1707/001-008). hUCB-MSCs were isolated and cultured according to a previously described method [18]. Briefly, human cord blood samples were mixed with a HetaSep solution (Stem Cell Technologies, Vancouver, Canada) at a ratio of 5:1 to remove red blood cells. The supernatants were subsequently placed on Lymphoprep (Stem Cell Technologies), and the mononuclear cells were separated after density-gradient centrifugation. The isolated cells were seeded in KSB-3 complete medium (Kangstem Biotech, Seoul, Republic of Korea) that contained 10% fetal bovine serum (FBS, Gibco BRL, Grand Island, NY, USA) and antibiotics. After 3 days of stabilization, unattached cells were removed, and isolated stem cells were retained.

Mast cell culture

The human MC line LAD2, which was kindly provided by Dr. D. D. Metcalfe of the Center for Cancer Research, National Institutes of Health (Bethesda, MD, USA), was cultured as previously described [2]. In brief, the cells were cultured in StemPro-34 serum-free medium (SFM) supplemented with 2 mM l-glutamine, 100 ng/mL recombinant human stem cell factor (rhSCF) and antibiotics. LAD2 cell granules were lysed by 5 freeze-thaw cycles, and cell debris was removed using a 0.2 μm syringe filter. Before the cells were utilized in experiments, the expression of cell-specific markers was verified by FACSCalibur flow cytometer and evaluated using

Cell Quest software (BD Bioscience, San Jose, CA, USA) (Figure S1).

Atopic dermatitis model induction in NC/Nga mice

All protocols related to the *in vivo* experiments were approved by the Seoul National University Institutional Animal Care and Use Committee (SNU-140320-1) and performed according to the committee guidelines. NC/Nga mice (male, 8 wks old) were obtained from SLC (Hamamatsu, Japan) and housed under specific pathogenic-free conditions at the animal facility of Seoul National University. AD-like symptoms were induced as described in previous studies [1, 19]. In brief, hair around the upper backs of the mice was shaved. The skin barrier was disrupted using 150 µL of 4% sodium dodecyl sulfate (SDS) treatment on the shaved dorsal skin and on both surfaces of each ear 3-4 h before the topical application of 100 mg of Df extract (Biostir Inc., Hiroshima, Japan). Df extract was applied twice per wk for three wks. To determine whether the functional improvement mediated by the pre-exposure of MC granules could specifically affect the therapeutic potential against AD, 1×10^6 hUCB-MSCs were subcutaneously infused on day 21 after 24 h of MC priming. The clinical severity was evaluated by scoring dryness, excoriation, erythema and edema (0, none; 1, mild; 2, moderate; 3, severe), with a maximum score of 12 [1]. After sacrifice on day 35, serum and dorsal skin samples were collected from the mice for further *ex vivo* examinations.

Histopathological evaluation

To investigate the histopathological changes in the lesions of Df-induced mice and excisional wounded mice, hematoxylin and eosin (H&E)-stained skin samples were subsequently analyzed. The collected skin samples were fixed in 10% formalin, prepared according to typical alcohol-xylene processes, and embedded in paraffin. Paraffin-embedded blocks were sectioned to a 5 µm thickness and stained with H&E or toluidine blue. Leukocyte infiltration was determined by H&E staining, MC infiltration and degranulation were assessed by toluidine blue staining.

Isolation of peripheral blood-derived mononuclear cells (PBMCs)

All experiments using human peripheral blood (PB) or PB-derived cells were approved by the IRB of Seoul National University (IRB no. 1707/001-008). To isolate PBMCs, blood samples were mixed with HetaSep solution (Stem Cell Technologies) at a ratio of 5:1. After incubation at room temperature for 1 h, the supernatant was carefully collected. PBMCs were separated using Lymphoprep (Stem Cell Technologies) density gradient centrifugation. Isolated cells were seeded in growth medium that consisted of RPMI 1640 (Gibco BRL) and 10% filtered FBS.

Mast cell degranulation

To explore the specific mechanism underlying the MC granule-mediated enhancement of the therapeutic effect on AD, IgE-mediated MC degranulation was determined as previously described [2]. Briefly, LAD2 cells were sensitized with 100 ng/mL human myeloma IgE (Millipore, Billerica, MA, USA) for 24 h. After 2 h of challenge with 10 µg/mL anti-IgE (Millipore), MC degranulation was halted on ice, and supernatants were harvested by centrifugation and assessed for β-hexosaminidase (β-hex) content. 60 µL of MC supernatant was mixed with an equal volume of substrate solution (7.5 mM ρ-nitrophenyl-N-acetyl-β-D-glucosaminide dissolved in 80 mM citric acid, pH 4.5). The mixture was incubated on a shaking incubator for 90 min at 37 °C, and 120 µL of 0.2 M glycine (pH 10.7) was then added. The absorbance at 450 nm was measured using a spectrophotometer (Tecan group, Mannedorf, Switzerland).

B cell isolation and analysis

To address whether MC-primed hUCB-MSCs directly affected the function of B cells, B lymphocytes were isolated from PBMCs using a naïve B cell isolation kit (Miltenyi Biotec, Bergisch Gladbach, Germany) according to the manufacturer's instructions. For B cell maturation, isolated cells were treated with 100 ng/mL CD154 (CD40 ligand) and 25 ng/mL IL-4 for 5 days. B cell maturation was analyzed by detecting surface or intracellular markers using flow cytometry. For surface marker staining, B cells were fixed and incubated with PerCP-conjugated anti-CD19, PE-conjugated anti-CD27 and FITC-conjugated anti-CD38. For intracellular marker staining, cells were fixed and permeabilized with an intracellular staining buffer set (BD Biosciences) and then incubated with a FITC-conjugated anti-IgE antibody after Fc receptor (FcR) blocking using an FcR blocking reagent (Miltenyi Biotec). Detection was performed with a FACSCalibur flow cytometer and evaluated using Cell Quest software (BD Bioscience).

Cell proliferation assay

After co-culture with hUCB-MSCs, the proliferation of human PBMCs, LAD2 cells and isolated B cells was measured using a bromodeoxyuridine (BrdU) ELISA kit according to the manufacturer's instructions. Briefly, the cells were

treated with 100 µM labeling reagent for more than 2 h. The cells were fixed and incubated in a peroxidase-conjugated anti-BrdU antibody (anti-BrdU-POD) solution and subsequently incubated with a tetramethyl benzidine (TMB) solution for 5 to 30 min. After a sufficient reaction time and addition of stop solution, the optical density (OD) was quantified by measuring the absorbance at wavelengths of 450 nm and 690 nm (as a reference) using a spectrophotometer (Tecan group).

Western blot analysis

Cell lysates of hUCB-MSCs were prepared with the protein lysis buffer Pro-prep (Intron Biotechnology Co., Seongnam, Republic of Korea) after the indicated treatments. The protein samples were separated by 10% SDS-PAGE and transferred to nitrocellulose membranes. After blocking with a 3% bovine serum albumin (BSA) solution, proteins on the membrane were incubated with primary antibodies against inducible nitric oxide synthase (iNOS), COX-2, galectin (Gal)-1, Gal-3 (Abcam, Cambridge, MA, USA), p-p38, p38, p-ERK1/2, ERK1/2, p-JNK1/2, JNK1/2, p-NF-κB and NF-κB (Cell Signaling Technology, Beverly, MA, USA) for more than 12 h at 4 °C and then incubated with secondary antibodies. Protein and antibody complexes were detected with enhanced chemiluminescence (ECL) reagent (GE Healthcare Life Science, Buckinghamshire, UK) and an analysis system.

Immunocytochemistry

After the indicated treatments, hUCB-MSCs were fixed with 4% paraformaldehyde (PFA) at room temperature for 10 min, permeabilized by incubation with a 0.05% Triton X-100 solution for 10 min and blocked with 5% normal goat serum (NGS) for 1 h. The cells were subsequently stained with specific primary antibodies against COX-2 (Abcam) and NF-κB (Cell Signaling Technology) followed by 2 h of incubation with Alexa 488- and Alexa 594-labeled secondary antibodies (1:1,000; Molecular Probes, Eugene, OR, USA), respectively. For counterstaining, nuclei were stained with DAPI. The images were captured by a confocal microscope (Nikon, Eclipse TE200, Tokyo, Japan).

Cytokine detection

IgE in the mouse serum was measured using a commercial ELISA kit (R&D Systems, Minneapolis, MN, USA). Culture supernatants of hUCB-MSCs were collected to determine the level of cytokines secreted from the cells. A commercial ELISA kit (R&D Systems) for PGE_2 was used according to the manufacturer's protocol. VEGF expression in the hUCB-MSCs cultured medium was assessed by cytometric bead array (CBA) human flex sets (BD Biosciences). Briefly, 50 µl of samples or standards were mixed with 50 µl of capture beads and incubated for 1 h. Then, 50 µl of a PE-conjugated detection antibody was added, and the mixture was incubated for an additional 1 h. Detection was performed with a FACSCalibur flow cytometer and evaluated using Cell Quest software (BD Bioscience).

Apoptosis assay

After co-culture with hUCB-MSCs, LAD2 cells were fixed with ice-cold 70% ethanol for 30 min and then incubated with RNase A (6.25 µg/ml) and propidium iodide (PI, 50 µg/ml) at 37 °C for 30 min. Cell cycle analysis was performed using a FACSCalibur flow cytometer and evaluated using Cell Quest software (BD Biosciences).

Calcium mobilization assay

The Fluo-3/AM calcium indicator (Invitrogen, Carlsbad, CA, USA) was employed to measure the intracellular calcium level in live hUCB-MSCs. The cells were cultured in confocal dishes (SPL, Pocheon, Republic of Korea) and washed with PBS before being treated with 5 µM Fluo-3/AM for 30 min and washed with PBS twice. The fluorescence intensities of the hUCB-MSCs treated with MC granules or histamine were measured at 488/515 nm every 1.6 s using a confocal microscope (Nikon). For analysis, the fluorescence intensities at each time point were normalized to the initial intensity and expressed as relative values (F/F_0).

Scratch wound assay

For collagen coating, 24-well cell culture plates were incubated with a 0.2 mg/ml type I collagen solution at 37 °C for 2 h. After rinsing with PBS twice, human keratinocyte HaCaT cells were seeded and maintained to attain 80% of the final density of the confluent monolayer. The cellular layer was subsequently scraped with a sterile pipette tip to make a 0.4-0.5 mm-wide-scratch. The culture medium was immediately replaced with a conditioned medium (CM) generated by hUCB-MSCs treated with MC granules or histamine, and spontaneous wound closure was impeded by the addition of 20 ng/ml IL-4 and IL-13. Wound closure was monitored for 12 h, and experiments were performed in triplicate.

Quantitative RT-PCR

After the designated treatments, total RNA was extracted from hUCB-MSCs using TRIzol reagent (Invitrogen). cDNA synthesis was performed using Superscript™ III reverse transcriptase (Invitrogen) and quantitative real-time PCR was performed using SYBR-Green PCR Master Mix and an ABI 7300

sequence detection system. The mRNA levels of each gene were normalized to those of the housekeeping gene GAPDH.

Excisional wound splinting model

All protocol related to *in vivo* experiments were approved by the Seoul National University Institutional Animal Care and Use Committee (SNU-140320-1) and performed in accordance with the committee guidelines. Excisional wound assays were conducted according to the protocol established by Wang et al. [20]. BALB/c mice (male, 8 wks old) were obtained from Orientbio (Seongnam, Republic of Korea). After a sufficient stabilization period, the mice were anesthetized and hair around their upper backs was shaved. The next day, the dorsal skin was punched with a 5-mm-diameter biopsy punch, and 1×10^6 MC-primed hUCB-MSCs were immediately infused subcutaneously at 4 sites around the wound. Silicone splints were fixed with instant-bond adhesive and a 6.0 nylon suture to prevent inadequate skin contraction. The wounds were completely covered with Tegaderm (3M) sterile transparent dressing and a self-adhering elastic bandage. The wound size was evaluated for 2 wks. After sacrifice on day 14, dorsal skin samples were collected from the mice for further *ex vivo* examinations.

Immunohistochemistry

For detection of CD31 expression, 5-μm-thick paraffin-embedded sections of skin were deparaffinized and rehydrated. For permeabilization, the samples were incubated with a 0.05% Triton X-100 solution at room temperature for 10 min and blocked with a 5% NGS for 1 h. Then, the cells were stained with anti-mouse CD31 monoclonal antibody (Abcam) overnight at 4 °C and secondary antibody labeled with Alexa Fluor 488 (Molecular Probes) for 1 h. Before imaging, nuclei were counterstained with DAPI. The images were captured by a confocal microscope (Nikon).

Statistical analysis

All results are expressed as the mean ± SD. Statistical analysis was performed using GraphPad Prism version 8.0 software (GraphPad Software, San Diego, CA, USA). All data were tested for normality by D'Agostino and Pearson normality tests. For normally distributed data, the significance was determined by Student's t tests for comparison of two groups or by one-way ANOVA coupled with Bonferroni's test for multiple groups. For non-normally distributed data, the Mann-Whitney U test or the Kruskal-Wallis method coupled with Dunn's multiple comparison test was used. P-values less than 0.05 were considered statistically significant and are indicated in the text.

Results

Generation of AD-specific hUCB-MSCs by priming with MC granules

We first investigated whether treatment with MC granules could alter the properties of hUCB-MSCs. Compared to those in the conditioned medium (CM) and cell contents (CC) of PBMCs and the CM of MCs, MC granules significantly increased the expression level of COX-2 but not those of the other factors known to be involved in immunoregulation (p<0.0001, Figure 1A). The upregulation of COX-2 expression was confirmed by immunostaining (Figure 1B) and assessing the subsequent secretion of PGE_2 (p=0.0172, Figure 1C). Activation of the COX-2~PGE_2 axis improves self-renewal and the immunosuppressive property of hUCB-MSCs. MC granule-mediated stimulation of the COX-2~PGE_2 signaling pathway resulted in an increased growth rate of hUCB-MSCs (p<0.0001, Figure 1D). In addition, the cells treated with MC granules suppressed the mitogen-induced proliferation of PBMCs more efficiently than naïve cells (p=0.0006, Figure 1E).

The therapeutic efficacy of hUCB-MSCs against AD is improved by pretreatment with MC granules

We subcutaneously injected MC-primed hUCB-MSCs into Df-induced AD mice and assessed the therapeutic efficacy. The symptoms of Df-treated mice were not significantly altered by the injection of hUCB-MSCs (p=0.0755, Figure 2A-B). However, the clinical severity of disease was significantly mitigated in mice treated with MC-primed cells (p=0.0010, Figure 2A-B). Upon histopathological assessment, we observed that skin damage, including edema with widened intercellular spaces in the epidermis and infiltration of lymphocytes in the perivascular region, were attenuated in the MC-preconditioned cell treated group (Figure 2C). Quantification of the data confirmed that mice treated with MC-primed hUCB-MSCs showed a 71.52% epidermal thickness compared to that of the naïve cell-treated group (p=0.0183, Figure 2C-D). Although exocytosis in the dorsal skin of Df-induced mice was not significantly attenuated by the administration of hUCB-MSCs (p=0.1255), MC-primed cells markedly suppressed lymphocytes by preventing their infiltration in the skin by more than 14.3% compared to that in naïve cells (Figure 2C and 2E).
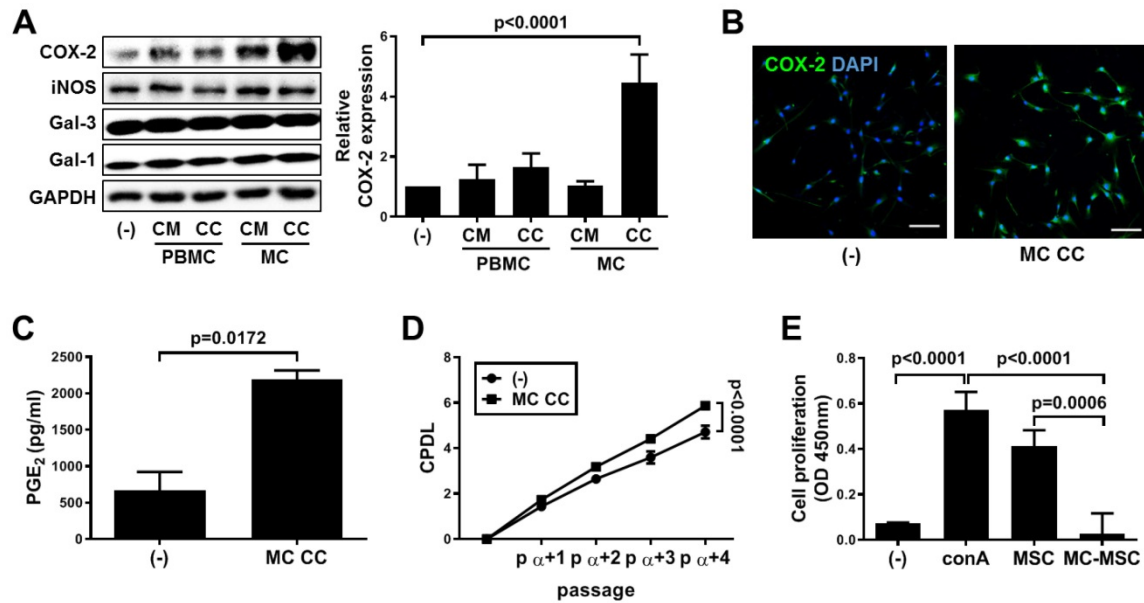
Figure 1. Priming with MC granules enhances the proliferation and immunosuppression of hUCB-MSCs. (A-C) MC granules were isolated from LAD2 cells and added to hUCB-MSC culture medium for 24 h. **(A)** The expression of the immune modulating factors COX-2, iNOS, Galectin (Gal)-1 and Gal-3 was detected by western blot analysis and quantified. **(B)** The expression of COX-2 in MC primed hUCB-MSCs was verified via immunostaining, bar = 100 μm. **(C)** Secretion of PGE₂ in the culture medium was determined by ELISA. **(D)** The accumulated changes in proliferation were measured by CPDL analysis. **(E)** Immunosuppressive properties of primed hUCB-MSCs were determined by the MLR assay. *In vitro* experiments were performed in triplicate using hUCB-MSCs isolated from each different donor (N=3). The results are shown as the mean ± SD.
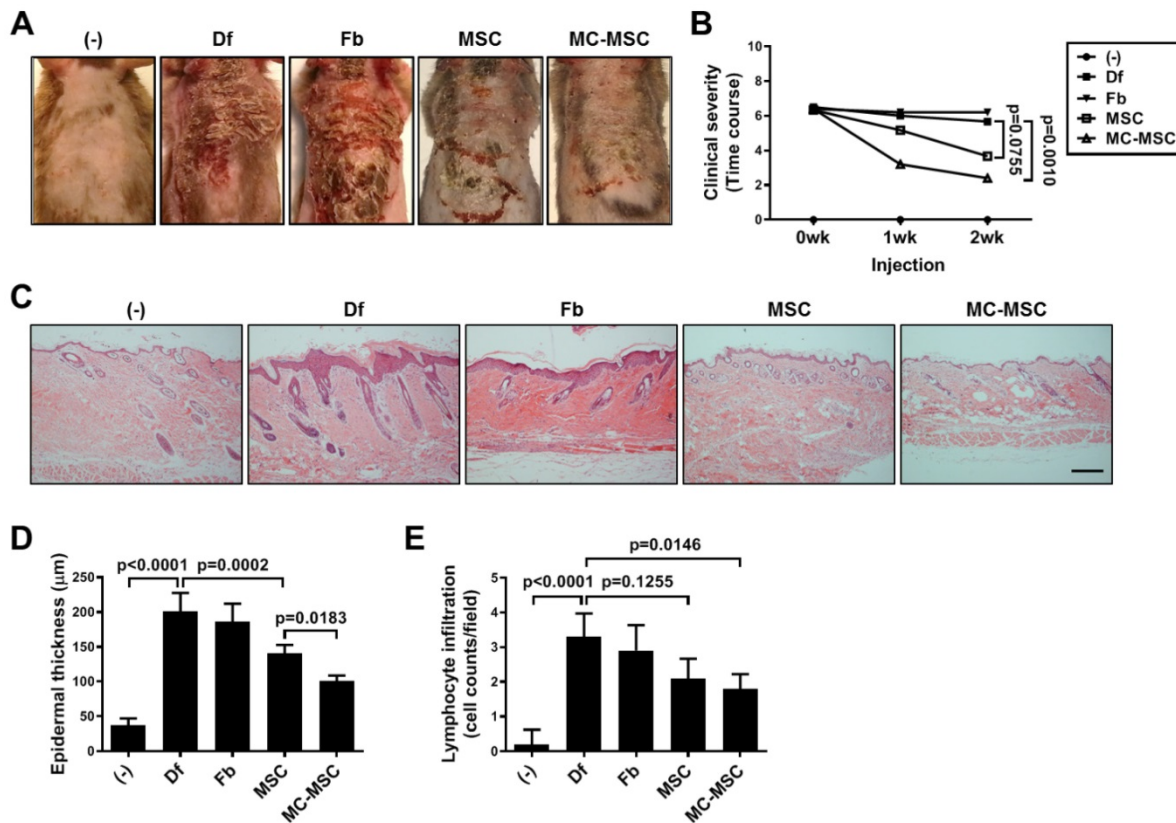

Figure 2. MC-primed MSCs attenuate symptoms of experimental atopic dermatitis more efficiently than naïve cells. NC/Nga mice were experimentally induced with atopic dermatitis (AD) by repetitive exposures to *dermatophagoides farinae* (Df) extract in the dorsal region. Each group of mice was monitored and sacrificed on day 35 for further *ex vivo* examinations. **(A)** Representative gross images of dorsal area lesions on the mice. **(B)** Clinical severity was assessed by scoring dryness, excoriation, erythema and edema (n=5-8). **(C)** Representative H&E-stained images of dorsal skin, bar = 500 μm. **(D-E)** Epidermal thickness **(D)** and lymphocyte infiltration **(E)** were measured from H&E-stained slides (n=5-8). (-): Negative control group, Df: Df-induced AD group, Fb: fibroblast-treated group, MSC: hUCB-MSC-treated group, MC-MSC: MC-primed hUCB-MSC-treated group. The results are shown as the mean ± SD.
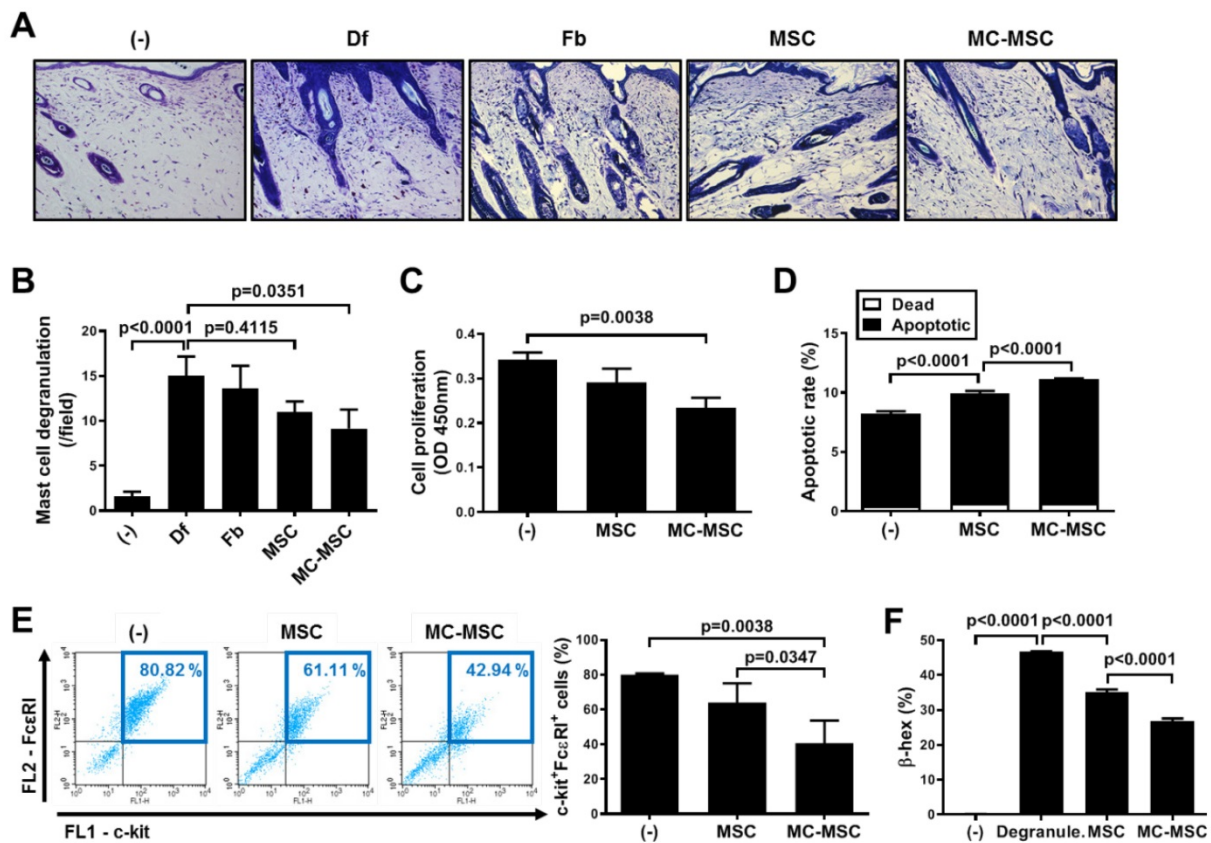
Figure 3. MC granules improve the suppressive effect of hUCB-MSCs on mast cell activation. (A-B) Mice were induced with experimental AD and skin samples were collected on day 35 for further *ex vivo* examinations. Representative toluidine blue-stained images of dorsal skin **(A)** and quantification of degranulating mast cells **(B)**; (n= 5-8), bar = 100 μm. (-): Negative control group, Df: Df-induced AD group, Fb: fibroblast-treated group, MSC: hUCB-MSC-treated group, MC-MSC: MC-primed hUCB-MSC-treated group. **(C-E)** LAD-2 cells were co-cultured with MC-primed hUCB-MSCs for 24 h. **(C)** The proliferation rate of LAD2 cells was assessed by the BrdU assay. Apoptosis **(D)** and the expression of cell surface markers **(E)** were determined by flow cytometric analysis. **(F)** After co-culture with hUCB-MSCs during the sensitization period (24 h), LAD-2 cells were challenged with anti-IgE (3 μg/ml). The degranulation rate of LAD2 cells was assessed by detecting β-hexosaminidase in the cultured medium. (-): Negative control group, Degranule.: degranualtion group, MSC: hUCB-MSC co-cultured group, MC-MSC: MC-primed hUCB-MSC co-cultured group. *In vitro* experiments were performed in triplicate, using hUCB-MSCs isolated from each different donor (N=3). The results are shown as the mean ± SD.

MC granule-primed hUCB-MSCs suppress the activation of MCs and B cells via the COX-2~PGE₂ axis

We next evaluated the number of degranulating MCs in the dorsal skin of mice. Naïve hUCB-MSCs slightly suppressed the degranulation of MCs, but not significantly (p=0.4115), while MC-primed cells showed a significantly decreased number of MCs (83.1% compared to that of naïve hUCB-MSCs, p=0.0351, Figure 3A-B). We further investigated whether pretreatment with MC granules could improve the suppressive effect of hUCB-MSCs on the function of MCs. The proliferation of LAD2 cells co-cultured with MC-primed hUCB-MSCs was decreased to 68.4% (p=0.0038, Figure 3C). In addition, the apoptosis of LAD2 cells was notably increased to 111.78% by co-culture with MC-primed hUCB-MSCs compared to that of naïve cells (p<0.0001, Figure 3D). The expression of c-kit and FcεRI, prominent markers of MCs, was halved by MC-primed hUCB-MSCs (p=0.0038, Figure 3E). In the same context, in *in vitro* analysis, co-culture with hUCB-MSCs inhibited the

degranulation of LAD2 cells (p<0.0001), and 8.18% of the suppressive effect was augmented by MC pretreatment (p<0.0001, Figure 3F).

We sought to determine whether MC granule treatment could exert a significant effect on the hUCB-MSC-mediated suppression of B cells. Unlike that in mice treated with naïve hUCB-MSCs (p=0.2675), the level of IgE in the sera of mice was significantly decreased by the administration of MC-primed hUCB-MSCs (86.3% compared to that in naïve hUCB-MSC-treated mice, p=0.0191, Figure 4A). Naïve B lymphocytes were isolated from PBMCs and cultured in the presence of growth factors, IL-4 and CD40L. The proliferation of B cells co-cultured with MC-primed hUCB-MSCs was remarkably reduced (63.2% compared to that of naïve hUCB-MSCs, p=0.0010, Figure 4B). Moreover, the maturation of B cells was hindered by hUCB-MSCs (p=0.0139), and this effect was amplified by 3.3-fold by MC granule treatment (p<0.0001, Figure 3C). Similar to the *ex vivo* analysis, B cells cultured with MC-primed hUCB-MSCs showed a more substantial decrease in

IgE expression than naïve hUCB-MSCs (74.4% compared to that in naïve hUCB-MSCs, p=0.0003, Figure 4D). We also discovered that hUCB-MSCs decreased the proportion of CD4+IL-4+ Th2 cells, as reported in previous reports, whereas this proportion in MC-primed MSCs was not significantly different from that in naïve cells (p=0.5800, Figure S2).

We next treated hUCB-MSCs with celecoxib, a selective COX-2 inhibitor, prior to co-culture with target cells. The mitogen-induced proliferation of PBMCs (p<0.0001, Figure S3A) and degranulation (p<0.0001, Figure S3B) of LAD2 cells were considerably retrieved by the treatment of MC-primed MSCs with celecoxib. Similar to that in the context of MCs, the decreased expression of maturation markers for B cells (p<0.0001, Figure S3C) and IgE (p=0.0022, Figure S3D) was restored by selective inhibition of COX-2.

Histamine stimulation via H_1 and H_4 receptors plays a crucial role in the MC granule priming-mediated immunosuppression of hUCB-MSCs

Histamine was dose-dependently administered to hUCB-MSCs. As a result, the expression of COX-2 (increased 2-fold, p=0.0183, Figure 5A) and the secretion of PGE_2 (increased 14.8-fold, p=0.0002, Figure 5B) were most distinctly increased at the concentration of 50 μM, which did not induce harmful changes (Figure S4). The increased level of COX-2 expression was confirmed by immunostaining (Figure 5C). Similar to that in the context of MC priming, histamine treatment improved the proliferation rate (p<0.0001, Figure 5D) and the immunoregulatory capacity (increased 1.67-fold compared with that of naïve hUCB-MSCs, p=0.0001, Figure 5E). In addition, the histamine-induced suppression of immune cells was retrieved by blocking the COX-2 signaling pathway as shown in MC priming (Figure S5). We sought to investigate which receptor subtypes were associated with upregulation of the COX-2~PGE_2 signaling pathway. The expression of the H_1, H_2 and H_4 subtype receptors was detected in hUCB-MSCs (Figure S6A). When the subtype receptor H_1 or H_4 was selectively inhibited, COX-2 expression was significantly decreased in the presence of MC granules (H1: 66.8% of that in MC-primed cells, p=0.0218 and H4: 36.37% of that in MC-primed cells, p=0.0007, Figure 5F) or histamine (H1: 55.8% of that in histamine treated cells, p=0.0039 and H4: 40.6% of that in histamine-treated cells, p=0.0003, Figure S6B), and the result was validated by determining the level of PGE_2 secretion (Figure 5G and Figure S6C).

MC granule-mediated phosphorylation of the MAPK and NF-κB signaling pathways upregulates COX-2 expression in hUCB-MSCs

We subsequently explored the mechanistic pathway that was influenced by MC granule or histamine treatment by evaluating the intracellular calcium mobilization after each treatment in hUCB-MSCs. The level of intracellular calcium was immediately provoked by treatment with MC granules or histamine (Figure 6A and supplementary videos 1 to 3). Moreover, treatment with MC granules triggered the phosphorylation of MAP kinases, p38, ERK1/2 and JNK1/2 in hUCB-MSCs (P-p38: P<0.0001, P-ERK1/2: P=0.0007 and P-JNK1/2: p=0.0208, Figure 6B-D). NF-κB, which plays a crucial role in amplifying COX-2 signaling, was subsequently activated in response to MC granules (p=0.0021, Figure 6E), and its nuclear translocation was verified by immunostaining (Figure 6F). Changes in the signaling pathways, including MAPK and NF-κB, were also observed when hUCB-MSCs were treated with histamine (Figure S7).
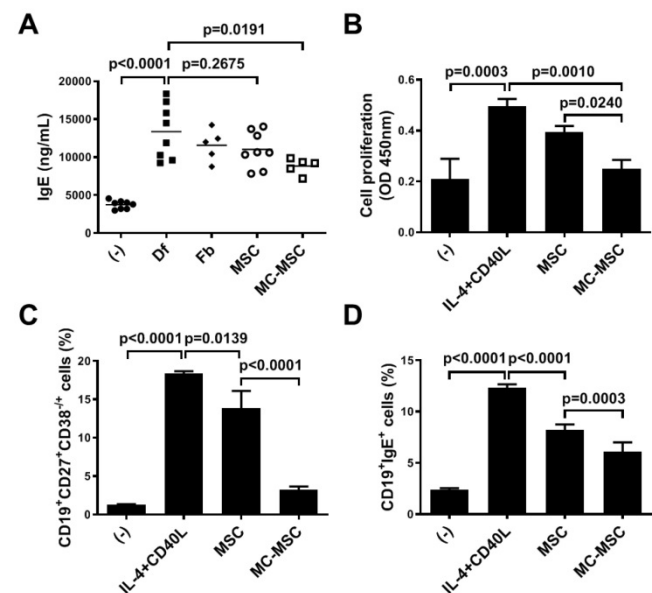

Figure 4. IgE production and maturation of B lymphocytes are efficiently suppressed by MC-primed hUCB-MSCs. (A) Mice were induced with experimental AD, and blood samples were collected on day 35 for further *ex vivo* examinations. The expression levels of IgE in the mouse sera were determined by ELISA (n=5-8). (-): Negative control group, Df: Df-induced AD group, Fb: fibroblast-treated group, MSC: hUCB-MSC-treated group, MC-MSC: MC-primed hUCB-MSC-treated group. **(B-D)** Naïve B lymphocytes were isolated from hPBMCs and cultured for 5 days in medium supplemented with CD40L (100 ng/ml) and IL-4 (25 ng/ml) in the presence of MC-primed hUCB-MSCs. **(B)** Proliferation of primary B lymphocytes was assessed by the BrdU assay. Maturation **(C)** and IgE production **(D)** were determined by flow cytometric analysis. (-): Negative control group, IL-4+CD40L: B cell maturation group, MSC: hUCB-MSC co-cultured group, MC-MSC: MC-primed hUCB-MSC co-cultured group. *In vitro* experiments were performed in triplicate, using hUCB-MSCs isolated from each different donor (N=3). The results are shown as the mean ± SD.
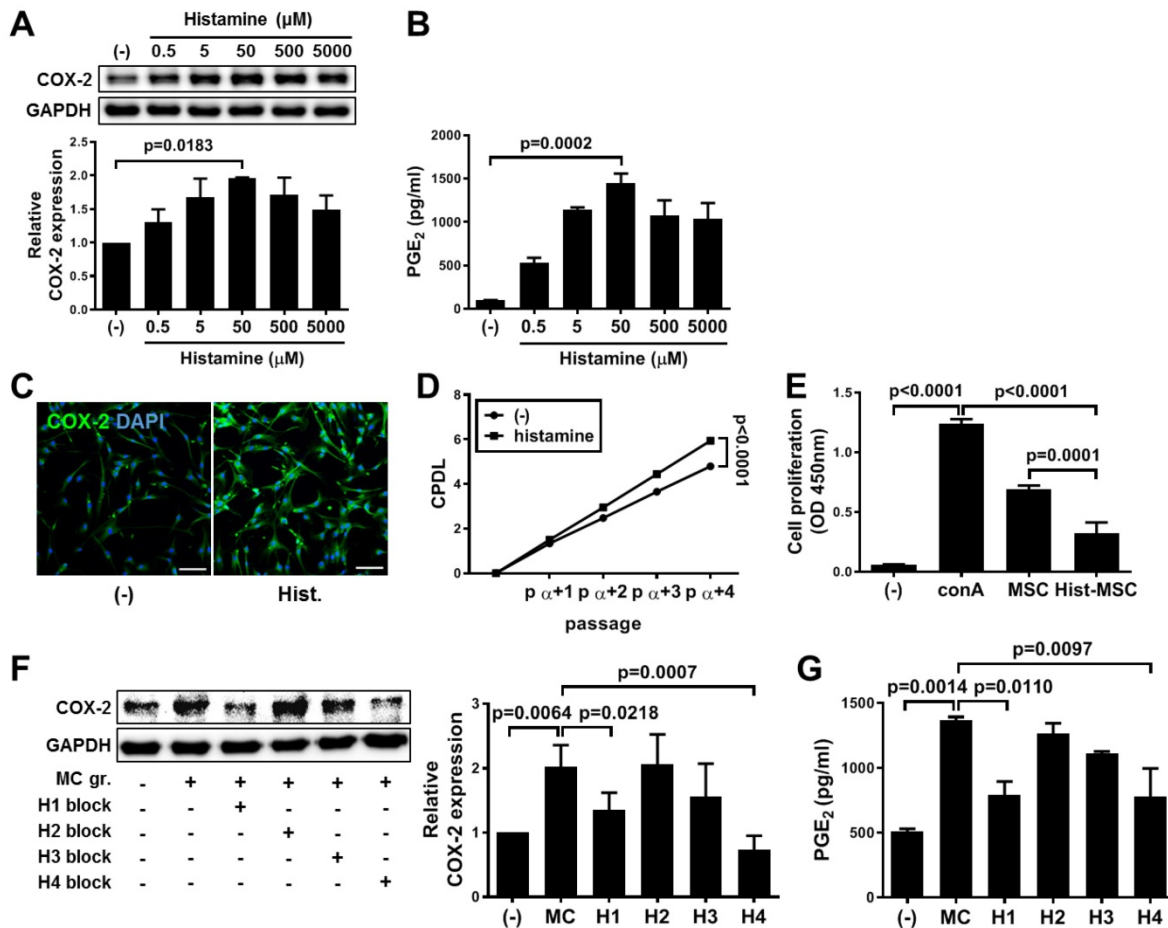
Figure 5. Upregulation of COX-2 signaling pathway in hUCB-MSCs mediated by histamine and its receptor subtypes 1 and 4. (A-B) hUCB-MSCs were treated with histamine dose-dependently for 24 h, and further experiments were conducted. The expression of COX-2 **(A)** and secretion of PGE$_2$ **(B)** were measured by western blot analysis and ELISA, respectively. **(C)** Immunocytochemistry of COX-2 expression in hUCB-MSCs after treatment with 50 μM histamine, bar = 100 μm. **(D)** The accumulated changes in proliferation were measured by CPDL analysis. **(E)** Immunosuppressive properties of histamine-treated hUCB-MSCs were determined by the MLR assay. **(F-G)** The inhibitory effects of subtype-specific antagonists of histamine receptors on the expression of COX-2 **(F)** and secretion of PGE$_2$ **(G)** were assessed by western blot analysis and ELISA, respectively. Blockers for H1: diphenhydramine hydrochloride, H2: cimetidine, H3: ciproxifan hydrochloride, H4: JNJ7777120. *In vitro* experiments were performed in triplicate, using hUCB-MSCs isolated from each different donor (N=3). The results are shown as the mean ± SD.

The wound healing ability of hUCB-MSCs is accelerated by MC granule treatment but not by histamine treatment

We next conducted an *in vitro* wound healing assay. The wound closure of human keratinocyte HaCaT cells was impeded by treatment with Th2 cytokines, IL-4 and IL-13 (67.8% of that in naïve HaCaT cells, p=0.0007), and CM from MC-primed hUCB-MSCs improved the recovery by 38 % compared with that of naïve hUCB-MSCs (p=0.0006, Figure 7A-B). In contrast, the CM of histamine-primed hUCB-MSCs was not significantly different from that of naïve cells (p>0.9999, Figure 7A-B). Furthermore, unlike histamine, MC granule priming notably augmented the expression of MCP-1 and the secretion of VEGF in hUCB-MSCs (MCP-1: increased 58.26-fold compared to that in naïve hUCB-MSCs, p=0.0067 and VEGF: increased 1.91-fold compared to that in naïve hUCB-MSCs, p=0.0012, Figure 7C-D). We verified our finding using an *in vivo* excisional wound healing model. Similar to the *in vitro* experiment, subcutaneously injected MC-primed hUCB-MSCs decreased the wound area by 20% more than that achieved with naïve MSCs on day 14 (p=0.0018, Figure 8A-B). In addition, as shown in Figure 7, cells treated with histamine were not significantly different from naïve cells (p=0.9618, Figure 8A-B). Upon histological assessment, we observed that granulation and immune cell infiltration were suppressed and re-epithelization was accelerated by the treatment of MC granule-primed hUCB-MSCs (Figure S8). Moreover, in the similar context with the secretion of VEGF from MC granule-treated hUCB-MSCs, the number of CD31-expressing capillary-like tubular structures increased in the skin of mice injected with MC granule-treated hUCB-MSCs (increased 3.18-fold compared to that in naïve hUCB-MSCs, p=0.0032, Figure 8C).
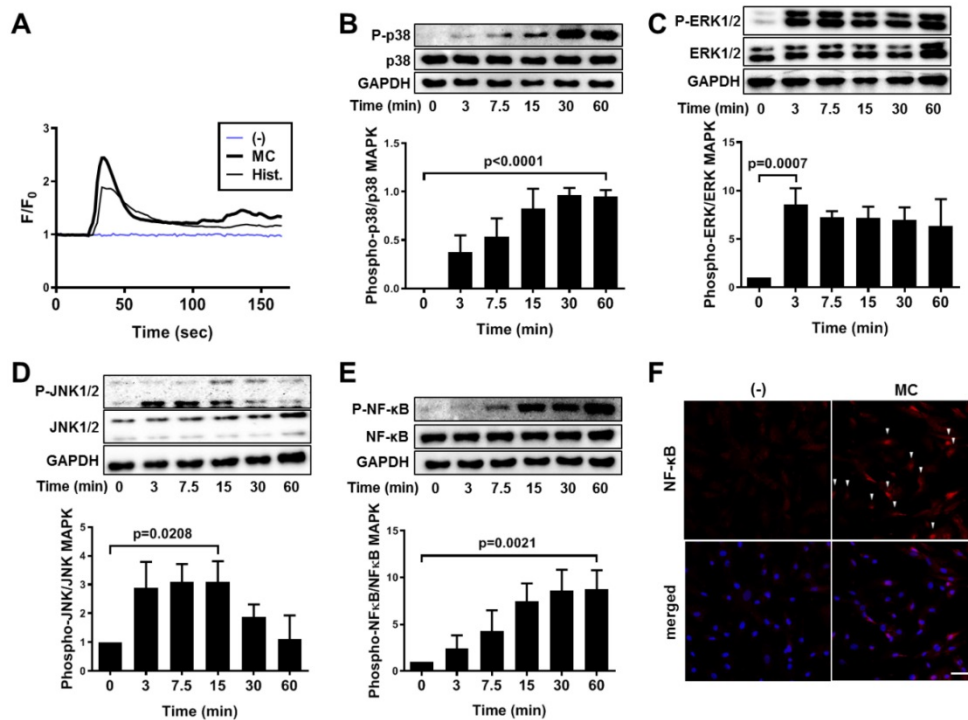
Figure 6. Histamine facilitates intracellular calcium mobilization and the NF-κB pathway in hUCB-MSCs to upregulate COX-2 signaling. (A) Ca^{2+} influx was detected in live cells treated with MC granules or histamine (50 μM) by staining with Fluo-3 AM. **(B-E)** hUCB-MSCs were treated with MC granules and cell lysates were collected at each indicated time point. Time-dependent phosphorylation of P(Thr^{180}/Tyr^{182})-p38 **(B)**, P(Thr^{202}/Tyr^{204})-ERK1/2 **(C)**, P(Thr^{183}/Tyr^{185})-JNK1/2 **(D)** and P(SER^{536})-NF-κB **(E)** in MC granule-primed hUCB-MSCs was determined by western blot analysis and quantified. **(F)** Immunocytochemistry analysis of NF-κB after treatment with MC granules, bar = 100 μm. *In vitro* experiments were performed in triplicate, using hUCB-MSCs isolated from each different donor (N=3). The results are shown as the mean ± SD.
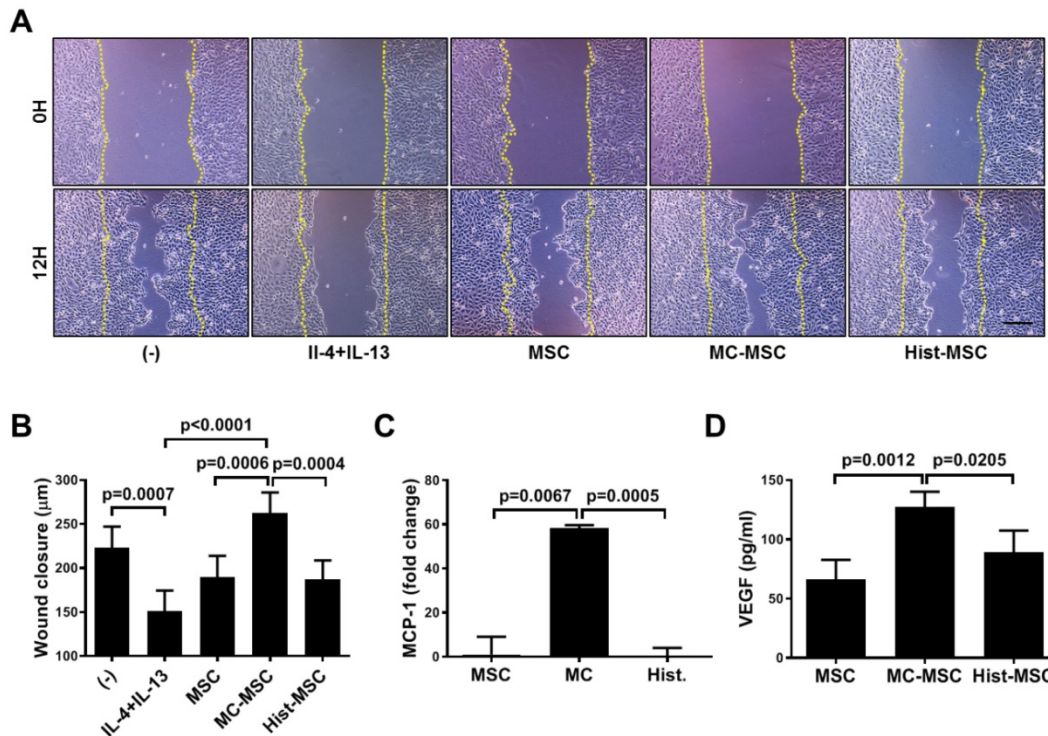

Figure 7. MC granules, but not histamine, promote the wound healing capacity of hUCB-MSCs *in vitro*. (A-B) Cells of the human keratinocyte line HaCaT were cultured until reaching 80% confluence and then scratched with a sterile pipette tip. The medium was immediately replaced with MC-MSC conditioned medium, and the wound gaps were measured for 12 h. Representative microscopic images of scratched HaCaT cells treated with conditioned medium from the indicated experimental groups **(A)** and quantification at 12 h **(B)**. **(C-D)** hUCB-MSCs were cultured in the presence of MC granules or 50 μM histamine and then, cell lysates and culture supernatants were collected for further assessment. **(C)** The expression of MCP-1 was assessed by qRT-PCR. **(D)** The secretion of VEGF was determined by cytometric bead array (CBA) analysis. *In vitro* experiments were performed in triplicate, using hUCB-MSCs isolated from each different donor (N=3). The results are shown as the mean ± SD.
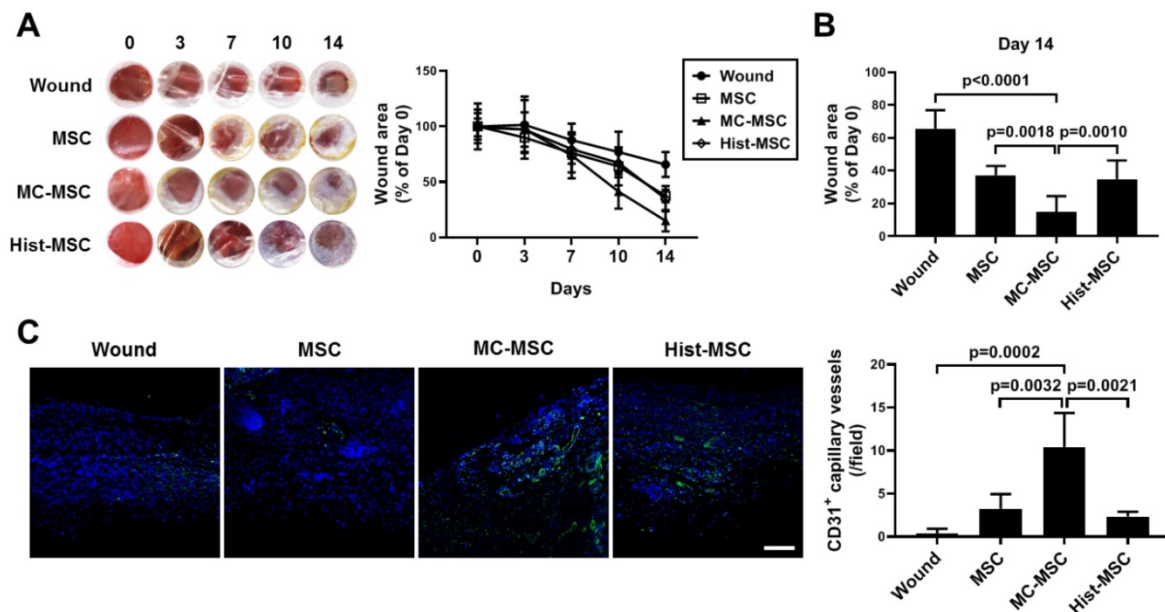
Figure 8. MC granule-primed hUCB-MSCs ameliorate excisional wound in the mice more efficiently than naïve and histamine-treated cells. The dorsal skin of BALB/c mice was punched with a 5-mm-diameter biopsy punch, and 1×10^6 MC-primed hUCB-MSCs were immediately infused subcutaneously. Each group of mice was monitored and sacrificed on day 14 for further *ex vivo* examinations. **(A)** Representative gross images of the wound area in the dorsal region and quantification of the wound size at each indicated time. **(B)** Detailed histogram for the quantification of the wound size on day 14. **(C)** Immunohistochemistry of CD31 expression in the dorsal skin of the mice (n=5), bar = 100 μm. Wound: Excisional wound mice group, MSC: hUCB-MSC-injected group, MC-MSC: MC-primed hUCB-MSC-injected group, Hist-MSC: histamine-treated hUCB-MSC-injected group. The results are shown as the mean ± SD.

Discussion

Although we reported a successful result from the clinical trial of treating moderate-to-severe AD with hUCB-MSCs [3], the development of a complementary method for actual cellular application will likely lead to better therapeutic outcomes and help overcome the current limitations, such as a donor-dependent variation [21]. Recent studies have suggested various enhancement strategies for stem cell therapy, including preconditioning with disease-related factors, such as TNF-α and IFN-γ [7, 22-24]. In line with these studies, we previously demonstrated that muramyl dipeptide (MDP), a constituent of the bacterial cell wall, plays a crucial role in promoting the immunomodulatory mechanism of hUCB-MSCs, and preconditioning with MDP significantly augmented the therapeutic efficacy of hUCB-MSCs against experimental colitis [25]. The crosstalk between the risk factors of a particular disease, including dysregulated activation of immune cells, and MSCs can be employed to identify its mode of action and develop disease-specific stem cell therapy [26]. In the present study, we have suggested priming with MC granules as a possible approach to enhancing stem cell-based therapy aimed at reducing skin inflammation and tissue degeneration in AD.

In this study, we showed that priming with MC granules enhances the proliferation and immunosuppressive properties of hUCB-MSCs by upregulating the COX-2~PGE$_2$ signaling pathway.

We next used gross and histological evaluations to validate the feasibility of the method by showing that the administration of MC granule-primed hUCB-MSCs alleviated the Df-induced AD-like symptoms in animal models more effectively than non-primed cells. For *in vivo* experiments, a polygenic NC/Nga mouse model and Df extract, an allergen, were employed. This animal AD model has been widely used for the assessment of the therapeutic potential of various alternative drugs, as AD-like symptoms, such as skin lesions, can be reproduced in these experimental animals [19, 27-30]. In addition, it is well known that the immune responses of mice, such as IgE hyperproduction in B cells [15] and degranulation of MCs [31], are similar to those of humans. We subsequently conducted comprehensive analyses to define the suppressive effect on each effector cell in the pathogenesis of AD. The activation of MCs, the major innate responder in an allergic reaction, is distinctly suppressed by hMSCs, which results in decreased degranulation, TNF-α production and SCF-mediated migration. This inhibition was shown to be largely mediated by the COX-2~PGE$_2$ signaling pathway [1, 32, 33]. In this study, we also showed that the number of degranulating MCs was considerably decreased by the subcutaneous administration of MC granule-primed hUCB-MSCs, and the inhibitory effect on MC degranulation was confirmed by *in vitro* experiments. We determined that MCs lost their surface expression of FcεRI by

co-culture with hUCB-MSCs, which presumably led to the decreased release of mediators. In addition, hUCB-MSCs pretreated with MC granules could more proficiently control the population of activated MCs by inducing apoptosis and regulating the expression of the constitutive receptor c-kit [34], which is essential for cellular growth. Our results suggest that preconditioning with MC granules augments the suppressive effect of hUCB-MSCs on MCs by not only directly inhibiting the degranulation but also by interrupting the robust proliferation of MCs.

MSCs have been reported to suppress excessive activation of effector B cells, such as memory B cells and plasmablasts, whereas they promote the regulatory type of B lymphocytes [2, 35, 36]. In the present study, the level of IgE was significantly diminished in only the sera of mice treated with MC-primed hUCB-MSCs. Through *in vitro* experiments, direct inhibition of hUCB-MSCs on IgE expression was validated. Interestingly, the suppression of maturation and IgE expression was improved by MC granule preconditioning and inversely abolished by the selective inhibition of COX-2. Similar to MCs, the proliferation of B lymphocytes was also influenced by MC-primed hUCB-MSCs. These findings suggest that the addition of MC mediators to the hUCB-MSC culture amplifies the immunomodulatory function to B cells and that the COX-2 signaling pathway plays a role in the suppression.

On the other hand, MC granule treatment did not induce any significant difference in the expression of IL-4, a prominent marker of Th2 cells, compared to that in naïve hUCB-MSCs. Given the previous reports that PGE_2 promotes the Th2 cell response [37, 38], these findings indicate that MC granule pretreatment and subsequent upregulation of the COX-2~PGE2 axis does not improve the suppressive effect on the development of Th2 cells.

Of note, histamine is well known as a pruritogen released from MCs in allergic disorders, including AD. In addition to its role in the itch response, histamine considerably contributes to the induction of skin inflammation by stimulating proinflammatory cells such as Th2 cells, eosinophils, MCs and M2a macrophages [39-42]. Histamine can synergize with the chemoattractant CXCL12 to promote the migration of MCs [43]. Moreover, histamine facilitates dendritic cells (DCs) to support T cell polarization toward the Th2 type by inhibiting the secretion of IL-12p70 and promoting the production of IL-6 and IL-10 in DCs [44]. In this study, we demonstrated that the MC granule-mediated upregulation of the COX-2 signaling pathway in hUCB-MSCs was associated with histamine. Histamine stimulated the COX-2

pathway and facilitated hUCB-MSCs to abrogate the abnormal activation of proinflammatory cells comparably to the MC mediator cocktail. Furthermore, we detected the same expression patterns of H_1, H_2 and H_4 receptors in hUCB-MSCs as those reported in bone marrow (BM)-derived MSCs [45]. According to our data, even in the presence of MC mediators or histamine, COX-2 expression and PGE_2 secretion were notably diminished by antagonization of the H_1 and H_4 receptors. We next questioned how histamine activated the COX-2 signaling pathway in hUCB-MSCs. Histamine is known to induce the mobilization of intracellular calcium and the activation of MAPKs [45, 46], which play a pivotal role in the stimulation of NF-κB and the subsequent COX-2 signal [47, 48]. In the present study, we showed that histamine could alter intracellular Ca^{2+} mobilization and lead to the phosphorylation of MAPK and NF-κB, as described in previous reports [45, 46, 49, 50]. Taken together, these results suggest that histamine, an MC granule component, plays a role in the COX-2-mediated immunomodulatory ability of hUCB-MSCs through the activation of its receptors H_1 and H_4 and the subsequent activation of the MAPK~NF-κB~COX-2 cascade.

To assess whether histamine could replace the MC priming pretreatment, we further investigated the differences between the cells of each group. In moderate-to-severe AD, sustained skin inflammation gradually disrupts the intact structure, resulting in the separation of keratinocytes and localized Th2 inflammatory responses; in particular, IL-4 impairs the spontaneous wound healing process. Consequently, a disease risk factor, impaired skin regeneration exacerbates the symptoms and prognosis of AD [51-53]. hMSCs are known to accelerate wound closure [54, 55]. As shown in the histological assessment, structural skin damage was observed in Df-induced mice, and the administration of MC-primed MSCs efficiently alleviated this defect. In the same context, the wound healing rate of keratinocytes was delayed by the addition of IL-4 and slightly increased by the CM of hUCB-MSCs. This rate was markedly increased by treatment with MC mediators but not by treatment with histamine. Wound healing is a complicated physiological phenomenon, and MSCs comprehensively contribute to the recovery process. MC granules upregulated the expression of VEGF and MCP-1 in hUCB-MSCs, which are essential for rebuilding the vasculature and chemoattraction in the damaged skin [56, 57]. The fact that MC granules contain numerous bioactive substances other than histamine [10] suggest that various factors related to the wound healing process

are influenced by priming with MC granules. In addition, we observed similar results from subsequent animal experiments. The CD31 expression in the mouse wound area was increased by the subcutaneous injection of MC-primed hUCB-MSCs, which supports the claim that improved VEGF secretion plays a role in accelerating the wound healing process. Taken together, these results suggest that hUCB-MSCs pretreated with MC granules ensure that keratinocytes more efficiently ameliorate tissue damage, while histamine does not contribute to the wound healing ability of hUCB-MSCs and thus cannot replace MC granule priming.

The present study revealed that preconditioning with MC granules enhanced the therapeutic potential of hUCB-MSCs against AD by improving the immunosuppression and tissue regenerative capacity of the cells. However, as the effect of MC pretreatment was verified in only animal models, the effect in the human body could be decided by clinical trials or corresponsive testing tools, considering differences from animals to humans, such as a species barrier. Next, regarding the wound healing effect, which types of granules are responsible for controlling the healing process remain to be determined. For the actual application of this method, simplification of the preparatory process and elimination of risk factors, such as the contamination of heterogeneous populations and microbial infection, are needed and related to the cost and labor. Therefore, elucidating the composition of a cocktail to serve as a substitute for MC granule is a future study goal. With these improvements, our findings might facilitate the development of a novel therapeutic strategy as well as expand our knowledge regarding the mechanisms of hMSC-based therapy for AD.

Supplementary Material

Supplementary figures.
http://www.thno.org/v09p3608s1.pdf
Supplementary Video 1.
http://www.thno.org/v09p3608s2.mp4
Supplementary Video 2.
http://www.thno.org/v09p3608s3.mp4
Supplementary Video 3.
http://www.thno.org/v09p3608s4.mp4

Abbreviations

AD: atopic dermatitis; BrdU: 5-bromo-2'-deoxyuridine; CC: cell contents; CD: cluster of differentiation; CM: conditioned medium; COX-2: cyclooxygenase-2; CPDL: cumulative population doubling level; Df: *dermatophagoides farinae*; hUCB-MSC: human umbilical cord blood-derived mesenchymal stem cell; IgE: immunoglobulin E; MAPK: mitogen-activated protein kinase; MC: mast cell; MCP-1: monocyte chemoattractant protein-1; MLR: mixed lymphocyte reaction; NF-κB: nuclear factor κ-light-chain-enhancer of activated B cells; PBMC: peripheral blood mononuclear cell; PGE$_2$: prostaglandin E$_2$; VEGF: vascular endothelial growth factor.

Acknowledgment

Competing Interests

The authors have declared that no competing interest exists.

References

1. Kim HS, Yun JW, Shin TH, Lee SH, Lee BC, Yu KR, et al. Human umbilical cord blood mesenchymal stem cell-derived PGE2 and TGF-beta1 alleviate atopic dermatitis by reducing mast cell degranulation. Stem Cells. 2015; 33: 1254-66.
2. Shin TH, Lee BC, Choi SW, Shin JH, Kang I, Lee JY, et al. Human adipose tissue-derived mesenchymal stem cells alleviate atopic dermatitis via regulation of B lymphocyte maturation. Oncotarget. 2017; 8: 512-22.
3. Kim HS, Lee JH, Roh KH, Jun HJ, Kang KS, Kim TY. Clinical Trial of Human Umbilical Cord Blood-Derived Stem Cells for the Treatment of Moderate-to-Severe Atopic Dermatitis: Phase I/IIa Studies. Stem Cells. 2017; 35: 248-55.
4. Park J, Kim B, Han J, Oh J, Park S, Ryu S, et al. Graphene oxide flakes as a cellular adhesive: prevention of reactive oxygen species mediated death of implanted cells for cardiac repair. ACS Nano. 2015; 9: 4987-99.
5. Lee BC, Shin N, Lee JY, Kang I, Kim JJ, Lee SE, et al. MIS416 Enhances Therapeutic Functions of Human Umbilical Cord Blood-Derived Mesenchymal Stem Cells Against Experimental Colitis by Modulating Systemic Immune Milieu. Front Immunol. 2018; 9: 1078.
6. Sah SK, Agrahari G, Nguyen CT, Kim YS, Kang KS, Kim TY. Enhanced Therapeutic Effects of Human Mesenchymal Stem Cells Transduced with Superoxide Dismutase 3 in a Murine Atopic Dermatitis-Like Skin Inflammation Model. Allergy. 2018.
7. Su W, Wan Q, Huang J, Han L, Chen X, Chen G, et al. Culture medium from TNF-alpha-stimulated mesenchymal stem cells attenuates allergic conjunctivitis through multiple antiallergic mechanisms. J Allergy Clin Immunol. 2015; 136: 423-32 e8.
8. Polchert D, Sobinsky J, Douglas G, Kidd M, Moadsiri A, Reina E, et al. IFN-gamma activation of mesenchymal stem cells for treatment and prevention of graft versus host disease. Eur J Immunol. 2008; 38: 1745-55.
9. Liu FT, Goodarzi H, Chen HY. IgE, mast cells, and eosinophils in atopic dermatitis. Clin Rev Allergy Immunol. 2011; 41: 298-310.
10. Kawakami T, Ando T, Kimura M, Wilson BS, Kawakami Y. Mast cells in atopic dermatitis. Curr Opin Immunol. 2009; 21: 666-78.
11. Heo SC, Jeon ES, Lee IH, Kim HS, Kim MB, Kim JH. Tumor necrosis factor-alpha-activated human adipose tissue-derived mesenchymal stem cells accelerate cutaneous wound healing through paracrine mechanisms. J Invest Dermatol. 2011; 131: 1559-67.
12. Hou Y, Ryu CH, Jun JA, Kim SM, Jeong CH, Jeun SS. IL-8 enhances the angiogenic potential of human bone marrow mesenchymal stem cells by increasing vascular endothelial growth factor. Cell Biol Int. 2014; 38: 1050-9.
13. Fan H, Zhao G, Liu L, Liu F, Gong W, Liu X, et al. Pre-treatment with IL-1beta enhances the efficacy of MSC transplantation in DSS-induced colitis. Cell Mol Immunol. 2012; 9: 473-81.
14. Silva LHA, Antunes MA, Dos Santos CC, Weiss DJ, Cruz FF, Rocco PRM. Strategies to improve the therapeutic effects of mesenchymal stromal cells in respiratory diseases. Stem Cell Res Ther. 2018; 9: 45.
15. Matsuda H, Watanabe N, Geba GP, Sperl J, Tsudzuki M, Hiroi J, et al. Development of atopic dermatitis-like skin lesion with IgE hyperproduction in NC/Nga mice. Int Immunol. 1997; 9: 461-6.

16. Karuppagounder V, Arumugam S, Thandavarayan RA, Sreedhar R, Giridharan VV, Pitchaimani V, et al. Naringenin ameliorates skin inflammation and accelerates phenotypic reprogramming from M1 to M2 macrophage polarization in atopic dermatitis NC/Nga mouse model. Exp Dermatol. 2016; 25: 404-7.

17. Izumi R, Azuma K, Izawa H, Morimoto M, Nagashima M, Osaki T, et al. Chitin nanofibrils suppress skin inflammation in atopic dermatitis-like skin lesions in NC/Nga mice. Carbohydr Polym. 2016; 146: 320-7.

18. Lee BC, Kim HS, Shin TH, Kang I, Lee JY, Kim JJ, et al. PGE2 maintains self-renewal of human adult stem cells via EP2-mediated autocrine signaling and its production is regulated by cell-to-cell contact. Sci Rep. 2016; 6: 26298.

19. Yamamoto M, Haruna T, Yasui K, Takahashi H, Iduhara M, Takaki S, et al. A novel atopic dermatitis model induced by topical application with dermatophagoides farinae extract in NC/Nga mice. Allergol Int. 2007; 56: 139-48.

20. Wang X, Ge J, Tredget EE, Wu Y. The mouse excisional wound splinting model, including applications for stem cell transplantation. Nat Protoc. 2013; 8: 302-9.

21. Kang I, Lee BC, Choi SW, Lee JY, Kim JJ, Kim BE, et al. Donor-dependent variation of human umbilical cord blood mesenchymal stem cells in response to hypoxic preconditioning and amelioration of limb ischemia. Exp Mol Med. 2018; 50: 35.

22. Kavanagh DP, Suresh S, Newsome PN, Frampton J, Kalia N. Pretreatment of Mesenchymal Stem Cells Manipulates Their Vasculoprotective Potential While Not Altering Their Homing Within the Injured Gut. Stem Cells. 2015; 33: 2785-97.

23. Duijvestein M, Wildenberg ME, Welling MM, Hennink S, Molendijk I, van Zuylen VL, et al. Pretreatment with interferon-gamma enhances the therapeutic activity of mesenchymal stromal cells in animal models of colitis. Stem Cells. 2011; 29: 1549-58.

24. Kwon YW, Heo SC, Jeong GO, Yoon JW, Mo WM, Lee MJ, et al. Tumor necrosis factor-alpha-activated mesenchymal stem cells promote endothelial progenitor cell homing and angiogenesis. Biochim Biophys Acta. 2013; 1832: 2136-44.

25. Kim HS, Shin TH, Lee BC, Yu KR, Seo Y, Lee S, et al. Human umbilical cord blood mesenchymal stem cells reduce colitis in mice by activating NOD2 signaling to COX2. Gastroenterology. 2013; 145: 1392-403 e1-8.

26. Ravanidis S, Bogie JFJ, Donders R, Deans R, Hendriks JJA, Stinissen P, et al. Crosstalk with Inflammatory Macrophages Shapes the Regulatory Properties of Multipotent Adult Progenitor Cells. Stem Cells Int. 2017; 2017: 2353240.

27. Sung YY, Yoon T, Jang JY, Park SJ, Jeong GH, Kim HK. Inhibitory effects of Cinnamomum cassia extract on atopic dermatitis-like skin lesions induced by mite antigen in NC/Nga mice. J Ethnopharmacol. 2011; 133: 621-8.

28. Takano N, Arai I, Kurachi M. Analysis of the spontaneous scratching behavior by NC/Nga mice: a possible approach to evaluate antipruritics for subjects with atopic dermatitis. Eur J Pharmacol. 2003; 471: 223-8.

29. Takaoka A, Arai I, Sugimoto M, Honma Y, Futaki N, Nakamura A, et al. Involvement of IL-31 on scratching behavior in NC/Nga mice with atopic-like dermatitis. Exp Dermatol. 2006; 15: 161-7.

30. Takeshita S, Tokunaga T, Tanabe Y, Arinami T, Ichinose T, Noguchi E. Asian sand dust aggregate causes atopic dermatitis-like symptoms in Nc/Nga mice. Allergy Asthma Clin Immunol. 2015; 11: 3.

31. Kotani M, Matsumoto M, Fujita A, Higa S, Wang W, Suemura M, et al. Persimmon leaf extract and astragalin inhibit development of dermatitis and IgE elevation in NC/Nga mice. J Allergy Clin Immunol. 2000; 106: 159-66.

32. Brown JM, Nemeth K, Kushnir-Sukhov NM, Metcalfe DD, Mezey E. Bone marrow stromal cells inhibit mast cell function via a COX2-dependent mechanism. Clin Exp Allergy. 2011; 41: 526-34.

33. Su WR, Zhang QZ, Shi SH, Nguyen AL, Le AD. Human gingiva-derived mesenchymal stromal cells attenuate contact hypersensitivity via prostaglandin E2-dependent mechanisms. Stem Cells. 2011; 29: 1849-60.

34. Cruse G, Metcalfe DD, Olivera A. Functional deregulation of KIT: link to mast cell proliferative diseases and other neoplasms. Immunol Allergy Clin North Am. 2014; 34: 219-37.

35. Franquesa M, Mensah FK, Huizinga R, Strini T, Boon L, Lombardo E, et al. Human adipose tissue-derived mesenchymal stem cells abrogate plasmablast formation and induce regulatory B cells independently of T helper cells. Stem Cells. 2015; 33: 880-91.

36. Luz-Crawford P, Djouad F, Toupet K, Bony C, Franquesa M, Hoogduijn MJ, et al. Mesenchymal Stem Cell-Derived Interleukin 1 Receptor Antagonist Promotes Macrophage Polarization and Inhibits B Cell Differentiation. Stem Cells. 2016; 34: 483-92.

37. Kalinski P. Regulation of immune responses by prostaglandin E2. J Immunol. 2012; 188: 21-8.

38. O'Garra A, Arai N. The molecular basis of T helper 1 and T helper 2 cell differentiation. Trends Cell Biol. 2000; 10: 542-50.

39. Mommert S, Gregor K, Rossbach K, Schaper K, Witte T, Gutzmer R, et al. Histamine H2 receptor stimulation upregulates TH2 chemokine CCL17 production in human M2a macrophages. J Allergy Clin Immunol. 2018; 141: 782-5 e5.

40. Thangam EB, Jemima EA, Singh H, Baig MS, Khan M, Mathias CB, et al. The Role of Histamine and Histamine Receptors in Mast Cell-Mediated Allergy and Inflammation: The Hunt for New Therapeutic Targets. Front Immunol. 2018; 9: 1873.

41. Cowden JM, Zhang M, Dunford PJ, Thurmond RL. The histamine H4 receptor mediates inflammation and pruritus in Th2-dependent dermal inflammation. J Invest Dermatol. 2010; 130: 1023-33.

42. Ehling S, Rossbach K, Dunston SM, Stark H, Baumer W. Allergic inflammation is augmented via histamine H4 receptor activation: The role of natural killer cells in vitro and in vivo. J Dermatol Sci. 2016; 83: 106-15.

43. Godot V, Arock M, Garcia G, Capel F, Flys C, Dy M, et al. H4 histamine receptor mediates optimal migration of mast cell precursors to CXCL12. J Allergy Clin Immunol. 2007; 120: 827-34.

44. Thurmond RL, Gelfand EW, Dunford PJ. The role of histamine H1 and H4 receptors in allergic inflammation: the search for new antihistamines. Nat Rev Drug Discov. 2008; 7: 41-53.

45. Nemeth K, Wilson T, Rada B, Parmelee A, Mayer B, Buzas E, et al. Characterization and function of histamine receptors in human bone marrow stromal cells. Stem Cells. 2012; 30: 222-31.

46. Razali NA, Nazarudin NA, Lai KS, Abas F, Ahmad S. Curcumin derivative, 2,6-bis(2-fluorobenzylidene)cyclohexanone (MS65) inhibits interleukin-6 production through suppression of NF-kappaB and MAPK pathways in histamine-induced human keratinocytes cell (HaCaT). BMC Complement Altern Med. 2018; 18: 217.

47. Diaz MF, Vaidya AB, Evans SM, Lee HJ, Aertker BM, Alexander AJ, et al. Biomechanical Forces Promote Immune Regulatory Function of Bone Marrow Mesenchymal Stromal Cells. Stem Cells. 2017; 35: 1259-72.

48. Yang IH, Wong JH, Chang CM, Chen BK, Tsai YT, Chen WC, et al. Involvement of intracellular calcium mobilization in IL-8 activation in human retinal pigment epithelial cells. Invest Ophthalmol Vis Sci. 2015; 56: 761-9.

49. Jain R, Watson U, Saini DK. ERK activated by Histamine H1 receptor is anti-proliferative through spatial restriction in the cytosol. Eur J Cell Biol. 2016; 95: 623-34.

50. Nizamutdinova IT, Dusio GF, Gasheva OY, Skoog H, Tobin R, Peddaboina C, et al. Mast cells and histamine are triggering the NF-kappaB-mediated reactions of adult and aged perilymphatic mesenteric tissues to acute inflammation. Aging (Albany NY). 2016; 8: 3065-90.

51. Li C, Lasse S, Lee P, Nakasaki M, Chen SW, Yamasaki K, et al. Development of atopic dermatitis-like skin disease from the chronic loss of epidermal caspase-8. Proc Natl Acad Sci U S A. 2010; 107: 22249-54.

52. Serezani APM, Bozdogan G, Sehra S, Walsh D, Krishnamurthy P, Sierra Potchanant EA, et al. IL-4 impairs wound healing potential in the skin by repressing fibronectin expression. J Allergy Clin Immunol. 2017; 139: 142-51 e5.

53. Zhao Y, Bao L, Chan LS, DiPietro LA, Chen L. Aberrant Wound Healing in an Epidermal Interleukin-4 Transgenic Mouse Model of Atopic Dermatitis. PLoS One. 2016; 11: e0146451.

54. Zhang B, Wang M, Gong A, Zhang X, Wu X, Zhu Y, et al. HucMSC-Exosome Mediated-Wnt4 Signaling Is Required for Cutaneous Wound Healing. Stem Cells. 2015; 33: 2158-68.

55. An Y, Liu WJ, Xue P, Ma Y, Zhang LQ, Zhu B, et al. Autophagy promotes MSC-mediated vascularization in cutaneous wound healing via regulation of VEGF secretion. Cell Death Dis. 2018; 9: 58.

56. Chen L, Tredget EE, Wu PY, Wu Y. Paracrine factors of mesenchymal stem cells recruit macrophages and endothelial lineage cells and enhance wound healing. PloS one. 2008; 3: e1886.

57. Hong KH, Ryu J, Han KH. Monocyte chemoattractant protein-1–induced angiogenesis is mediated by vascular endothelial growth factor-A. Blood. 2005; 105: 1405-7.